

A Binary Collision Model for Plasma Simulation with a Particle Code

TOMONORI TAKIZUKA

Japan Atomic Energy Research Institute, Tokai, Ibaraki, Japan

AND

HIROTADA ABE

Department of Electronics, Kyoto University, Kyoto, Japan

Received May 24, 1976; revised October 28, 1976

A binary collision model by the Monte Carlo method is proposed for plasma simulations with particle codes. The model describes a collision integral of the Landau form. Collisional effects in spatially uniform plasmas are simulated, and the results are in good agreement with theoretical ones.

1. INTRODUCTION

Computer simulations of plasmas with particle codes play important roles in the research of transport phenomena, heating processes, and so on. In these simulations, the number of particles is far smaller than that in the simulated situations, because of the limitation of speed and capacity of the computer. The result is that fluctuation phenomena such as collisions are greatly enhanced. In order to reduce the collisional effects, the finite-size particle model has been introduced [1]. The properties of a plasma of finite-size particles have been studied by many authors [2-4]. The phenomena occurring for wavelengths longer than the size of a cloud are unchanged by the use of the finite-size particle model, while the short-wavelength modes are not accurately simulated. In usual simulations, the cloud size is chosen to be on the order of the Debye radius, and the properties of binary collisions are changed. Especially in one and two-dimensional simulations, the effects of collisions are much different from those in real plasmas.

Accordingly, it is appropriate to introduce a method for adding the effects of binary collisions into the finite-size particle model, when collisional effects in a plasma are studied. Shanny *et al* [5] introduced Lorentz gas collision model into a one-dimensional electron plasma simulation. By the use of this model, Tsang *et al* [6] studied the neoclassical diffusion in a toroidal magnetic field. Lorentz gas collision model, however, simulates only the electron-ion collisions. Gula and Chu [7] used the Krook

model in the simulation of the two-stream instability. Takizuka et al. [8] performed the simulation of the plasma confinement in a toroidal quadrupole, in which a collision model was introduced by utilizing a modification of Langevin's equation. The procedure for adding the effects of binary collisions developed by Oliphant and Nielson [9] is that the scattering angle is given on the basis of the local collision frequency, in these models, however, the collision frequencies do not have any velocity dependence. On the other hand, Monte Carlo methods in which a collision between two particles is directly simulated have been used to study shock waves in neutral gases [10, 11], and the results are in excellent agreement with available experimental data.

In this paper, we propose a binary collision model by a Monte Carlo method for plasma simulations with particle codes. In Section II, the model is described. In Section III, computer simulations of spatially uniform plasmas are performed to check the model.

II. MODEL

In order to simulate the effects of binary collisions in a plasma, we introduce a binary collision model by a Monte Carlo method for a particle simulation. At first, we explain the major steps in the model. Next the detailed descriptions of some steps are presented.

Major Steps

The major steps in the model are as follows.

- (1) The configuration of simulated boundaries is applied, and the region is divided into a number of spatial cells with dimension such that the change in plasma properties across each cell is small.
- (2) The initial state of a plasma is specified, i.e., the initial position and velocity of each particle are set up.
- (3) Time is advanced by discrete steps of magnitude Δt , sufficiently small compared with the mean relaxation time.
- (4) The particle motion and the collision processes, are considered to be uncoupled over the time interval Δt , and the former is calculated with the finite-size particle method.
- (5) Particles are grouped at every cell: all cells are numbered and particles are arranged in the addresses by the cell number.
- (6) Pairs of particles suffering binary collisions are determined at random in a cell, because the finite separation of particles in a cell is neglected in this model. The pairs consist of three kinds; two ions, two electrons, and an ion and an electron.
- (7) The changes in the velocities of two particles due to a binary collision in the time interval Δt are computed.

(8) The velocity of each particle is replaced by the new one given by the above calculation.

(9) Steps (3)-(8) are repeated successively.

Grouping of Particles

Now we explain a method to group particles at every cell (Step (5)).

(i) All cells are numbered from 1 to J .

(ii) The number of particles M_j in the cell j is counted: the total number is $N = \sum M_j$.

(iii) A particle, which is placed at the address n ($1 \leq n \leq N$) and is contained in the cell j , is marked with the cell number j_n .

(iv) Preparing N dummies, we replace the dummy $n' = N + 1 + (n-1)/M_j$ by the particle n , where N is the number of particles in cells from 1 to $j-1$.

(v) After all dummies are replaced by particles, the particle n is replaced by the dummy n . Then particles are arranged in the addresses by the cell number.

When the total number of particles is large, particles may be stored on disks, and a small fraction of the particles are in the fast memory. For such a case, a method to group particles is proposed as follows. We consider a two-dimensional (2-D) simulation in which the simulated region is divided into $M \times M$ cells.

(i) The region is also divided into K subregions which consist of $m \times m$ cells, respectively ($M^2 = Km^2$), and a cell in the subregion k is numbered as $j = (k-1)M + i$ ($1 \leq i \leq m^2$).

(ii) Initially, all particles contained in the subregion k are in the fast memory: their number is about N/K .

(iii) Motions of them are calculated by the finite-size particle method in the time interval Δt , and some particles go out to other subregions: their number is about $(1/2m) N/K$, when $v_t \Delta t$ is nearly equal to the cell length.

(iv) The particles remaining in k are stored on the disk A , and the particles escaping from k are stored on the disk B .

(v) These steps, (ii)-(iv), are repeated until k is equal to K . At last, the number of particles stored on the disk B is about $(K/2m) N \ll K$.

(vi) The particles on the disk B are arranged in the addresses by the subregion number, by the use of the method mentioned above.

(vii) At the next time step, we can easily take out particles contained in the subregion k from the disks A and B to the fast memory.

(viii) When $K/2m$ is larger than unity, we prepare the disk B , ($1 < K/2m \leq 1 + K/2m$) and take out particles from the disks A and B to the fast memory.

Determination of pairs

We grouped particles at every cell, and then we determine pairs of particles suffering binary collisions in a cell (Step (6)). We consider a situation such that M ions and N_e electrons exist in a cell at the time t . The ion density ρ_i and the electron density ρ_e are defined as $\rho_i = M/V$ and $\rho_e = N_e/V$, respectively, where $V = N/V_0$ (N_0 is the particle number in a cloud and V_0 is the cell volume) in a three-dimensional (3-D) simulation, or $\rho_i = n_i/S_0$ (n_i is the line density of a cloud and S_0 is the cell area) in a 2-D simulation, or $\rho_i = \rho_i/L_0$ (ρ_i is the surface density of a cloud and L_0 is the cell length) in a one-dimensional (1-D) simulation. At first we interchange the addresses of the memories in which the positions and velocities are stored, at random, as shown in Fig. 1. Next we determine pairs of particles suffering binary collisions.

Case 1a. Pairs of particles of the same species are determined in order from the top of the addresses, when the particle number is even, as shown in Fig. 2a.

Case 1b. If the particle number is odd, the first three particles are combined in three pairs (Fig. 2b).

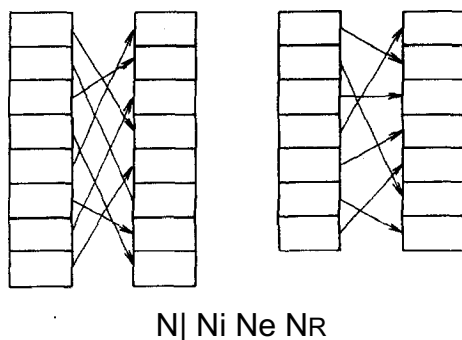


FIG. 1. Random replacement of the addresses of memories.

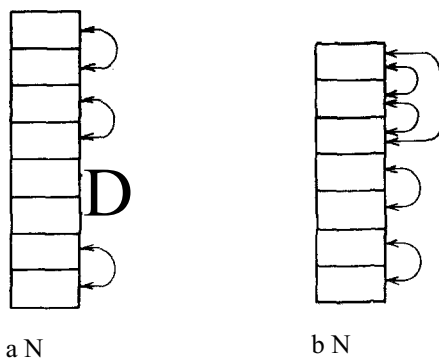


FIG. 2. Selection of pairs of the same species when N is even (a), (b) If N is odd, first three particles are combined in three pairs.

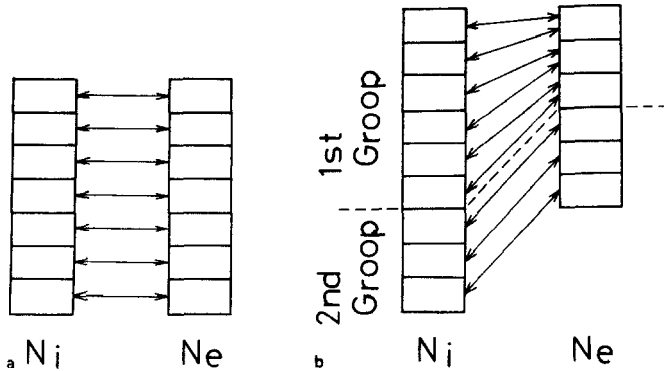


FIG. 3. Selection of pairs of an ion and an electron, (a) $M = N_e$, (b) $N_i > N_e$.

Case Ia. Pairs of an ion and an electron are chosen in order from the top of the addresses, when M is equal to N_e (Fig. 3a).

Case Ib. If M is greater than N_e ($M/N_e = i + r$, where z is a positive integer and $0 < r < 1$), ions and electrons are divided into two groups; ions of $(z+1)rN_e$ and electrons of rN_e (First group), and ions of $z(1-r)N_e$ and electrons of $(1-r)N_e$ (Second group). Each electron of the first is selected $z+1$ times for the pair to an ion of the first, and each electron of the second is chosen z times for the pair to an ion of the second (Fig. 3b). The same procedure is used when $N_i > M$.

Changes in Velocities

Thus we can determine pairs of particles at random in a cell. Next we calculate the changes in the velocities due to binary collisions in the time interval Δt (Steps (7) and (8)). As an example of a pair, one particle of species a with mass m_a and charge q_a has a velocity \mathbf{v}_a at the time t , and the other of species b with mass m_b and charge q_b has a velocity \mathbf{v}_b . The relative velocity in the laboratory frame defined as

$$\mathbf{M} = \mathbf{v}_b - \mathbf{v}_a = (u_x, u_y, u_z)^t \quad (1)$$

is transformed into that in the frame of the relative velocity at the time t :

$$\begin{pmatrix} \cos \theta \cos J & \cos J \sin \theta - \sin \theta \sin J & 0 \\ -\sin \theta & \cos \theta & 0 \\ \sin \theta \cos J & \sin \theta \sin J & \cos \theta \end{pmatrix} \begin{pmatrix} u_x \\ u_y \\ u_z \end{pmatrix}^t = \begin{pmatrix} 0 \\ 0 \\ u \end{pmatrix}^t, \quad (2)$$

where the angles θ and J are defined as shown in Fig. 4. As the result of a binary collision the magnitude of the relative velocity is unchanged but its direction is altered by the scattering angle θ as illustrated in Fig. 5:

$$(0, 0, u) \rightarrow (u \sin \theta \cos \phi, u \sin \theta \sin \phi, u \cos \theta), \quad (3)$$

where the angle ϕ takes on values from 0 to 2π . The postcollision relative velocity

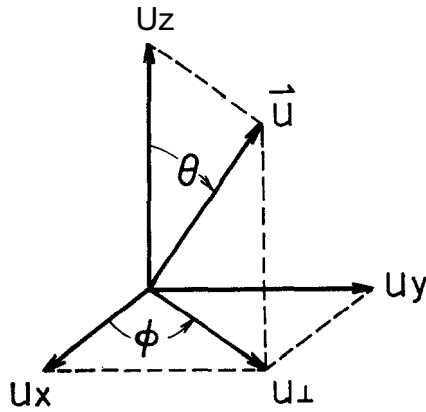


FIG. 4. Coordinates in the laboratory frame and the relative velocity u at the time t .

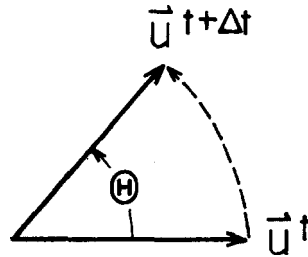


FIG. 5. The change in the relative velocity.

in the frame of the precollision relative velocity is transformed into that in the laboratory frame. It can be expressed in the form

$$(u_x, u_y, u_z) = (u_x^t, u_y^t, u_z^t) + \Delta u \quad (4a)$$

$$\Delta u_x = (u_x^t/u_{\perp}^t)u_z^t \sin \theta \cos \phi - (u_y^t/u_{\perp}^t)u_z^t \sin \theta \sin \phi + (1 - \cos \theta)u_x^t, \quad (4b)$$

$$\Delta u_y = (u_y^t/u_{\perp}^t)u_z^t (\sin \theta \sin \phi - (1 - \cos \theta)u_y^t/u_{\perp}^t), \quad (4c)$$

and

$$\Delta u_z = -u_z^t \sin \theta \cos \phi - u_z^t \sin \theta \sin \phi + (1 - \cos \theta)u_z^t, \quad (4d)$$

where $u_{\perp}^t = \sqrt{(u_x^t)^2 + (u_y^t)^2}$. Eqs. (4) are written in the form

$$\Delta u_x = w \sin \theta \cos \phi, \quad (4b')$$

$$\Delta u_y = w \sin \theta \sin \phi, \quad (4c')$$

and

$$\Delta u_z = -w(1 - \cos \theta). \quad (4d')$$

By the use of these expressions we obtain the postcollision velocity of the particle α and that of the particle β ;

$$\mathbf{v}_\alpha^{t+\Delta t} = \mathbf{V}_j + (\text{加}/\%) / u \quad (5a)$$

and

$$\text{豪}'' = \mathbf{v}_j - \mathbf{J}u, \quad (m_{\alpha\beta}/m_\beta) \quad (5b)$$

where the reduced mass w_{a0} is defined by

$$W_{a0} = m_\alpha m_\beta / (m_\alpha + \text{加}8). \quad (6)$$

It is easily seen that both total momentum and total energy are conserved for a collision. In order to give the scattering angle in Eqs. (4), we introduce the relations

$$\sin \theta = 28/(1 + 8^2) \quad (7a)$$

and

$$1 - \cos \theta = 28^2/(1 + 3^2). \quad (7b)$$

The variable $\theta \equiv \tan(\theta/2)$ is chosen randomly with the Gaussian distribution. The mean is zero and the variance $\langle \text{承} \rangle$ is given by

$$\langle \text{斗} \rangle = (e_a^2 e / 77 \epsilon_0 A / 87 T e_0^{2\wedge 2} w^3) 4, \quad (8a)$$

where ϵ_0 is the permittivity of vacuum, n_L is the lower density between $\%$ and n_0 , and A denotes the Coulomb logarithm [12]. In the case that the particle number N_a is odd and the first three particles are combined in three pairs (Case ib), the variance $\langle 8^2 \rangle$ for the first three collisions is given by

$$\langle \text{斗} \rangle = 8(q_a^2 m_\alpha / \text{力}) \quad (8b)$$

In a simulation the time step is finite, and the value of $\langle S^2 \rangle$ proportional to Δt and to 加^2 becomes larger than unity occasionally. In this case, the scattering angle θ is chosen randomly with a uniform distribution between 0 and 大

Remarks

These operations are performed over the all pairs of particles in the time interval Δt , and each particle suffers collisions with an ion (or some ions, in Case Ib and Case lib) and with an electron (or some electrons). The random selection of the pair to a test particle from field particles through many time steps are approximately equivalent to an integration of the distribution function for field particles, in the case that the time interval is sufficiently small compared with the relaxation time [13]. Accordingly, the collision term in the kinetic equation for the particles which suffer collisions described by this model is given in the Landau form:

$$\frac{\partial f_\alpha}{\partial t} = - \frac{e_\alpha^2 e_\beta^2 \lambda}{877 \epsilon_0^2 m_\alpha J I M W^3 J L \text{ 彻/ 加仪仇} \%} \left[\frac{u_j u_k}{m_\beta} \right] \left[\frac{\text{工筑}(\mathbf{v}')}{\% \langle \text{斗} \rangle \text{筑}} \right] \text{ 传) } .$$

III. RESULTS

In order to check the model, we perform simulations of spatially uniform plasmas. The simulated region is not divided into spatial cells, and the finite-size particle method is not used here.

Collision Frequencies [12, 14]

A test particle of species a with a velocity v_a (a energy % =加卢//2) is moved in a medium of field particles 机 which are distributed according to a Maxwellian distribution with temperature " :

$$九=啾恤/2\pi\pi \quad)^{3/2} \exp(-w_c r^2/27^{\wedge}). \quad (10)$$

We introduce the function $/z(x)$ and its derivative $M(x)$:

$$\mu(x) = (2/\#/2) r_{J_0} g Y f/2 \text{ 点} \quad (11a)$$

and

$$W(x) = (2/\炉/ \% 5 \text{ NG.} \quad (11b)$$

We can obtain the mean rate-of-change of velocity and energy of the test particle in the form

$$\langle dv_j \text{ 力} \rangle = - \text{镶} * \quad (12a)$$

with

$$\text{"肚} = (1 + \text{制秒初} 8 / \text{明} 7 \text{产然} 8 \sqrt{2} \text{色} 2 \text{加那} 2 \text{蝴} 2) \quad (12b)$$

and

$$\langle \text{鸡/力} \rangle = - \text{挈} \% \quad (13a)$$

with

$$\text{"*} = 2 \text{ [黑 L 时} 3 \text{'(x)一秒' (X)] 片他"} \text{ 8 A/277\%2破2碎}, \quad (13b)$$

where v_g and 吸 are called the "slowing-down frequency" and the "energy transfer frequency,** respectively, and x denotes $m_\beta \epsilon_\alpha / m_\alpha T_\beta$. The rate of the increase of spread in the velocity component transverse to the original direction can be written in the form

$$\langle \text{血心/今} \rangle = \text{唐} \% : \quad (14a)$$

with

$$\text{炉} = 2 \text{ 口(1) + W(x)-嘴] 步} * 0 / 0 2, \quad (14b)$$

where ω is the deflection frequency.^M The "energy-exchange frequency" ν_e is also introduced as the rate of the increase of the energy spread:

$$\langle d(\Delta \text{ 谢})/dt \rangle = \text{理综六} \quad (15a)$$

with

$$\nu_e^{\alpha/\beta} = 4 \frac{m_\alpha}{m_\beta} \mu(x) \frac{T_\beta}{\text{分}} \frac{e_\alpha^2 e_\beta^2 n_\beta \lambda}{8 \sqrt{2} \text{叫吧} 2 \sqrt{2} \cdot} \quad (15b)$$

The "total" collision frequencies $\nu_{\text{总}}$ $\nu_{\text{总}}$ $\nu_{\text{总}}$, and $\nu_{\text{总}}$ are derived from the "partial"

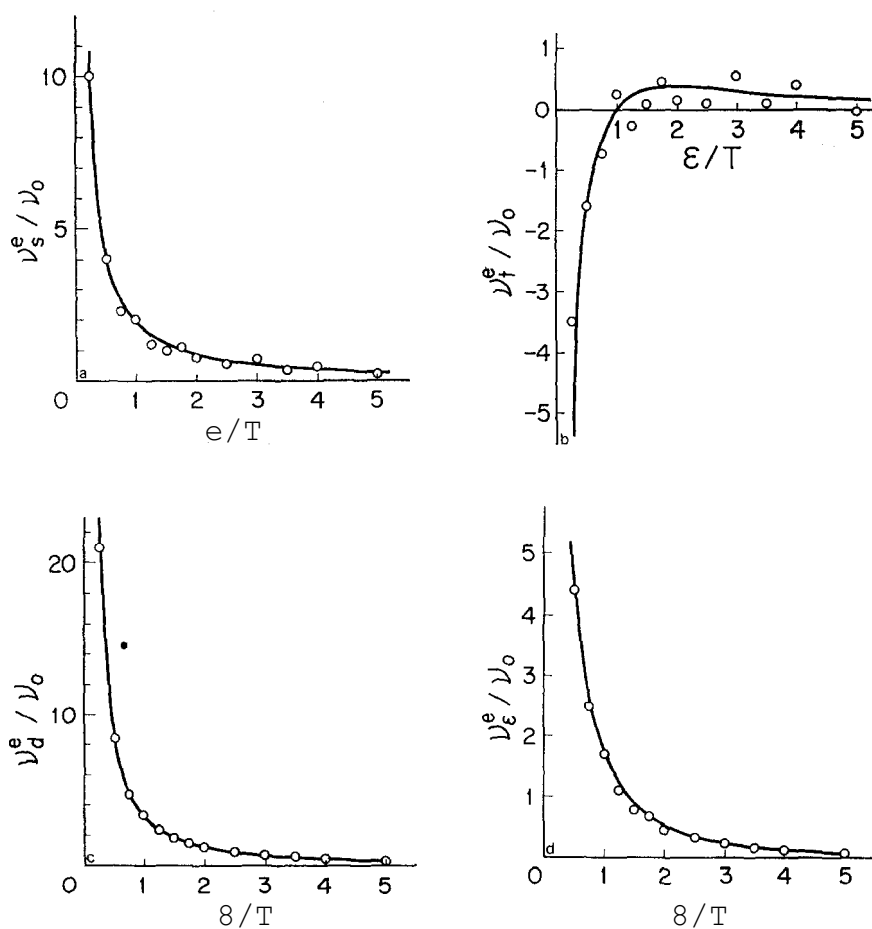


FIG. 6. (a) The electron "slowing-down frequency" ν_s^e , (b) the electron "energy transfer frequency" ν_t^e , (c) the electron "deflection frequency" ν_d^e , and (d) the electron "energy-exchange frequency" ν_e^e , functions of energy of the test particle. An open circle represents the ensemble average of 6×10^3 particles, and solid curves correspond to theoretical ones.

collision frequencies 吟巴 比% 吟巴 and 琛川:

$$\text{評}=\frac{\varepsilon}{3} \frac{W}{m^*}$$

(16)

We obtain the "total" collision frequencies in the simulation used the binary collision model. Simulation parameters are the following: $e\backslash = -e^{\textcircled{R}} = e$, $m^* = 1836m_e$, $m \sim n_e = n$, $T_i \sim T_e = T$, $N = W$ for each species, and $t = 10 \tau$ where the basic collision frequency % is defined as

$$= \frac{e^2 \text{加}}{4 \pi \epsilon_0 m^2 g^2 n^2 \lambda_D^2} \cdot$$

C7、
-.."

Figures 6 show the electron collision frequencies %* 也J 心气 and τ / as functions of

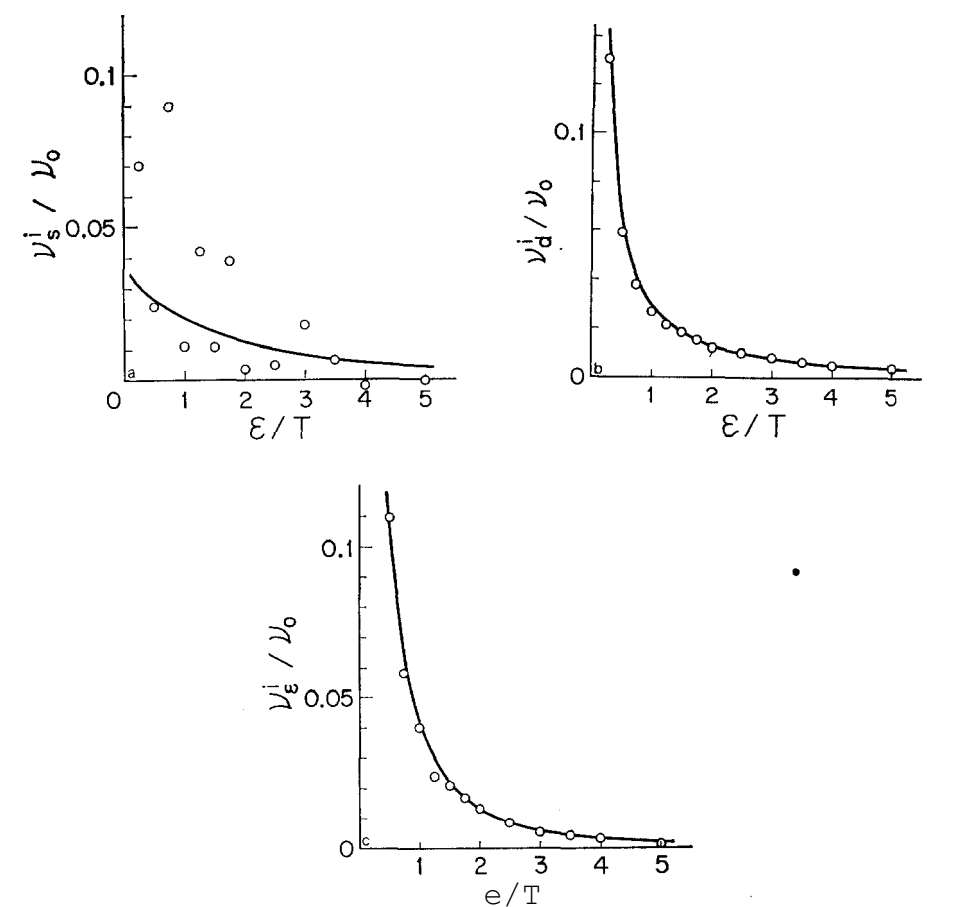


FIG. 7. (a) The ion ^slowing-down frequency" ν_s^i) the ion "deflection frequency" ν_d^i and (c) the ion ^energy-exchange frequency" ν_e^i .

energy of the test particle, and Figs. 7 show the ion collision frequencies ν_{ii} , ν_{ie} and r_i . An open circle in the figures represents the ensemble average of 6×10^3 particle $\bullet \Delta t$ and solid curves correspond to Eqs. (12)-(16). The "deflection frequencies" and the "energy-exchange frequencies" observed in the simulation are different from theoretical ones by several percent. Considering that the distribution of 10^3 particles deviates from a Maxwellian, these errors may be small enough. On the contrary, the errors in the "slowing-down frequencies"⁵⁷ and the "energy transfer frequencies" are not small. One of the causes of these errors is that the ensemble average is obtained by summing up many plus values and many minus values, and their absolute values are of the same order.

Relaxation Processes [12, 14]

We investigate macroscopic relaxation processes related to the "slowing-down frequency" and the "energy transfer frequency" J in which the errors are not small for the above observation.

We consider that electrons are distributed initially according to a shifted Maxwellian distribution with mean velocity v_{e0} and temperature T_{e0} , and that ion temperature is far smaller than $(7H_i/w_e)^{7/2}$. The time variation of the mean velocity v_e is given approximately by

$$d\langle v_e \rangle / dt = -r_s v_e, \quad (18a)$$

with

$$\nu_{ie} = 2(\nu_{ii} + \nu_{ie}) \quad (18b)$$

where w denotes $\sqrt{2}T_{e0}/m_e$. Simulations are performed on conditions: $w = T_{e0}/2$, $\nu_{ii} = \nu_{ie}$, and $\nu_{ie} = 2\nu_{ii}$. Other simulation parameters are the same as mentioned above. The solid curves in Figs. 8 are the results of simulations and dashed curves correspond to Eqs. (18). Figure 8a shows the statistical scatter in the results of three runs with the same parameter.

Next we consider the case that ion temperature T_{i0} and electron temperature T_{e0} are different initially. The equilibration of temperatures is expressed by equations

$$d(T_i - T_e)/dt = -2\nu_{ie}(T_i - T_e) \quad (19a)$$

with

$$\nu_{ie} = \frac{8 m_e}{m_i} \nu_{ii} \left(\frac{T_i}{T_e} \right)^{-3/2} \quad (19b)$$

The results of simulations are shown in Fig. 8a ($\nu_{ii}/\nu_{ie} = 4$, $T_{i0}/T_{e0} = 1$), Fig. 9b ($\nu_{ii}/\nu_{ie} = 4$, $T_{i0}/T_{e0} = 2$), and Fig. 9c ($\nu_{ii}/\nu_{ie} = 16$, $r_{i0}/r_{e0} = 1$).

The initial distribution with different longitudinal and transverse temperature (K_{\parallel} and T_{\perp}) is forced to an isotropic Maxwellian distribution. The rate of the relaxation is approximated by

$$d(T_{\parallel} - T_{\perp})/dt = f(1) - T_J \quad (20a)$$

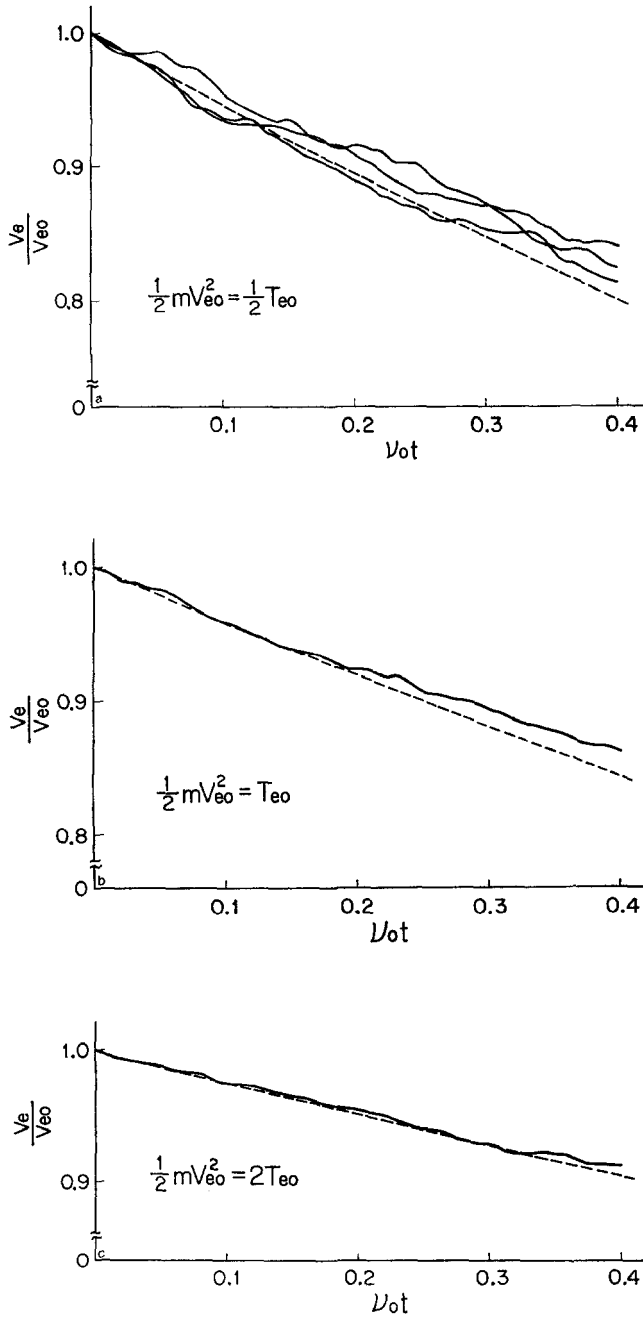


FIG. 8. The time variation of the electron mean velocity V_e . (a) $\epsilon = \frac{1}{2}T_{e0}$, (b) $\epsilon = T_{e0}$, (c) $\epsilon = 2T_{e0}$. The solid curves are the results of simulations and the dashed curves correspond to theoretical ones.

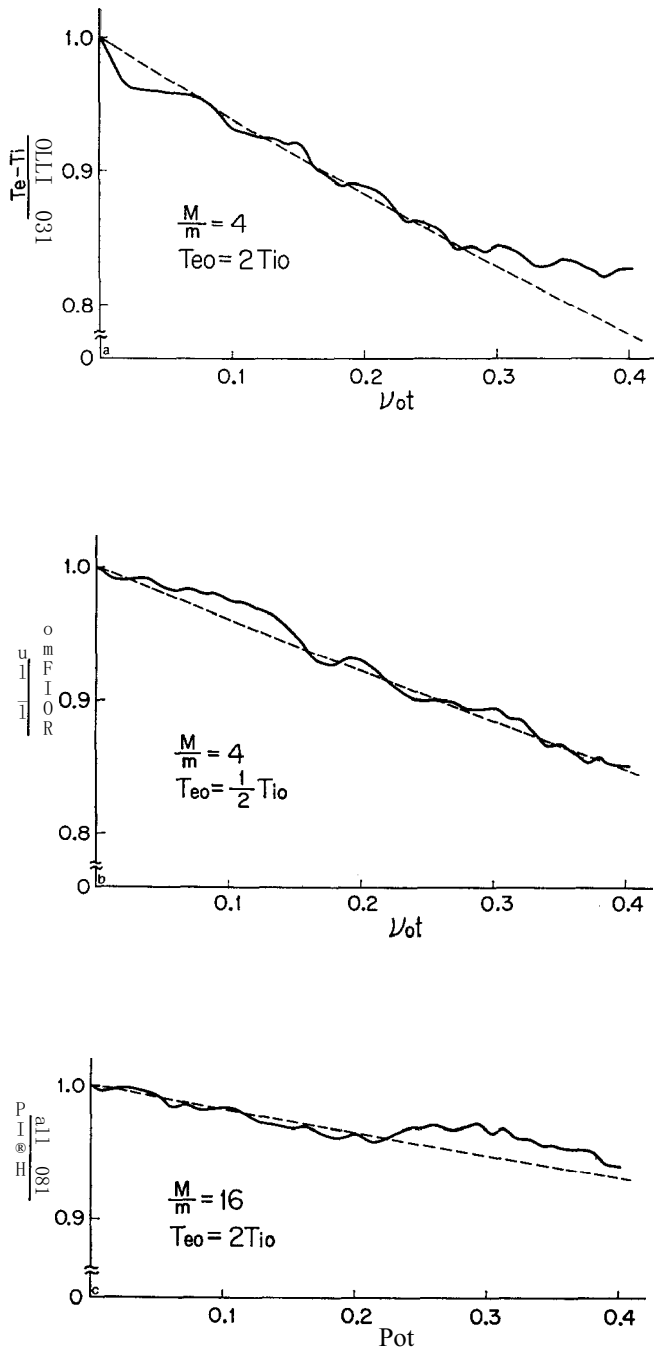


FIG. 9. The equilibration of ion temperature T_i and electron temperature T_e (a) $m_i/m_e = 4$, $T_{e0}/T_{i0} = \frac{1}{2}$, (b) $T_{e0}/T_{i0} = 2$, (c) $m_i/m_e = 16$, $T_{e0}/T_{i0} = \frac{1}{2}$.

with

$$\nu = (8/5(2\pi)^{-1/2})^{1/2} \%, \quad (20b)$$

where ν is given by introducing the relation $T = (T_{\parallel} + 2T_{\perp})/3$, and the condition $|T_{\parallel} - T_{\perp}| \ll T$ is assumed. Figure 10 shows the result of the simulation in case of $\nu_G \sim 27\%$.

The deviation from the isotropic distribution caused by statistical scatter is balanced with the relaxation mechanism by collisions, and forms itself into a small and un-growing fluctuation, as shown in Fig. 11.

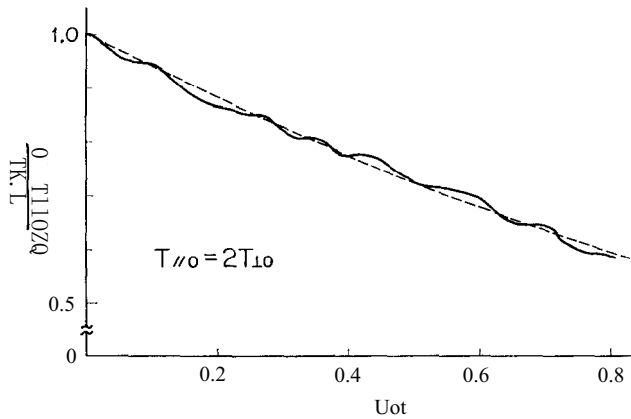


FIG. 10. The relaxation of the difference between longitudinal temperature and transverse one ($T_{\parallel 0} = 2T_{\perp 0}$).

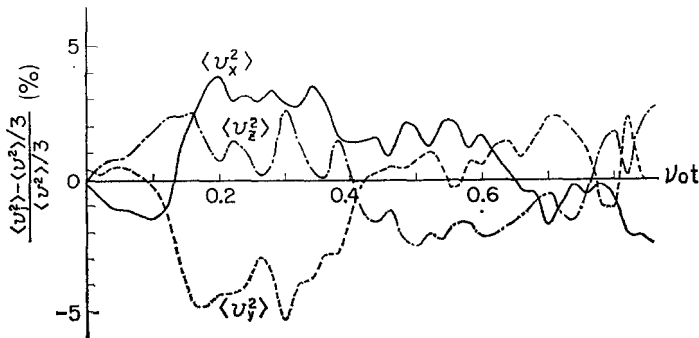


FIG. 11. The deviation from the isotropic distribution.

IV. SUMMARY AND DISCUSSION

We have proposed a binary collision model for plasma simulations with particle codes. The major procedures of the model are that (1) a particle suffers binary collisions in the time interval with an ion and an electron which are chosen randomly in a

spatial cell, and that (2) the change in the relative velocity results from a Coulomb interaction. The model conserves both total momentum and total energy, and it describes a collision integral of the Landau form.

The results of simulations of spatially uniform plasmas are in good agreement with the results obtained by theoretical analyses in which the Landau collision integral is used. However, the statistical scatter in the results is not avertible. This scatter is reduced by increasing the number of simulation particles.

Computation time is about 10^{-4} sec/particle • on the FACOM 230-75.

ACKNOWLEDGMENT

The authors wish to thank Professor H. Momota for his useful suggestions.

REFERENCES

1. C. K. BIRDSALL AND D. FUSSELL, *J. Computational Phys.* **3** (1969), 494.
2. A. B. LANGDON AND C. K. BIRDSALL, *Phys. Fluids* **13** (1970), 2115.
3. H. OKUDA AND C. K. BIRDSALL, *Phys. Fluids* **13** (1970), 2123; C. K. BIRDSALL, A. B. LANGDON, AND H. OKUDA, in "Methods in Computational Physics," Vol. 9, p. 241, Academic Press, New York, 1970.
4. Y. MATSUDA AND H. OKUDA, *Phys. Fluids* **18** (1975), 1740.
5. R. SHANNY, J. M. DAWSON, AND J. M. GREENE, *Phys. Fluids* **10** (1967), 1281.
6. K. T. TSANG, Y. MATSUDA, AND H. OKUDA, *Phys. Fluids* **18** (1975), 1282.
7. W. P. GULA AND C. K. CHU, *Phys. Fluids* **16** (1973), 1135.
8. T. TAKIZUKA, H. ABE, H. MOMOTA, AND C. NAMBA, *Plasma Phys.* **17** (1975), 887.
9. T. A. OLIPHANT AND C. W. NIELSON, *Phys. Fluids* **13** (1970), 2103.
10. J. K. HAVILLAND, in "Methods in Computational Physics," Vol. 4, p. 109, Academic Press, New York, 1965.
11. G. A. BIRD, in "Rarefied Gas Dynamics/* Vol. 1, p. 85, Academic Press, New York, 1969.
12. L. SPITZER, JR. "Physics of Fully Ionized Gases," Chap. 5, Interscience, New York, 1956.
13. G. A. BIRD, *Phys. Fluids* **13** (1970), 2676.
14. B. A. TRUBNIKOV, in "Reviews of Plasma Physics," Vol. 1, p. 105, Consultants Bureau, New York, 1965.